CHEMISTRY
A EUROPEAN JOURNAL

DOI: 10.1002/chem.200500166

Co-TUD-1: A Ketone-Selective Catalyst for Cyclohexane Oxidation

Mohamed S. Hamdy,[a] Anand Ramanathan,[b] Thomas Maschmeyer,[c] Ulf Hanefeld,*[b] and Jacobus C. Jansen*[a]

Abstract: Cobalt-containing mesoporous TUD-1 with different Si/Co ratios (100, 50, 20, and 10) was synthesized by the direct hydrothermal treatment method (DHT) using triethanolamine (TEA) as a template. The prepared samples (denoted as Co-TUD-1) were characterized by XRD, UV/Vis spectroscopy, elemental analysis, N_2 sorption measurements, ^{29}Si magic-angle spinning (MAS)-NMR, Raman spectroscopy, and HRTEM. The catalytic performance of Co-TUD-1 samples was tested in the liquid-phase oxidation of cyclohexane with *tert*-butylhydroperoxide (TBHP) as oxidant under solventless conditions. Higher catalytic efficiency was observed in samples with low Co-loading and thus, most likely isolated Co^{II} active sites, than in samples with high Co-loading and nanoparticles or bulk Co_3O_4 embedded in the TUD-1 silica.

Keywords: cobalt oxide · Co-TUD-1 · mesoporous materials · nanoparticles · oxidation

Introduction

The selective and efficient activation of paraffins and their conversion into valuable building blocks is a major scientific challenge. The successful, controlled oxidation of these unreactive substances to mono- or difunctionalized compounds is also of great economic significance. The conversion of cyclohexane to cyclohexanone [K] and cyclohexanol [A] with high selectivity is of importance as these compounds are utilized in the manufacture of nylon-6 and nylon-6,6.[1,2] Currently, conversions have to be kept well below 10% to achieve reasonable selectivities and to avoid overoxidation. For this selective oxidation of cyclohexane, cobalt is used as the principal metal in both homogeneous and heterogeneous catalysis. Industrially, this reaction is carried out homogeneously at temperatures above 150°C. A selectivity of approximately 85% for mono-oxygenated products (a mixture of K, A, and the intermediate cyclohexylhydroperoxide (CHHP)) is achieved. The CHHP is decomposed either directly or in a separate step to yield additional ketone and alcohol.[3,4] In a follow-up step, the cyclohexanol produced has to be converted into the desired product, cyclohexanone. Consequently, a heterogeneous system might offer several advantages, such as ease of separation, recycling of the catalyst, and solvent-free reaction conditions. Cobalt-containing molecular sieves have been extensively studied for their application in heterogeneous cyclohexane oxidation.[5–14] However, the K/A ratios reported in these studies were only around 1–2. It has been proven that the framework-substituted cobalt is responsible for the catalytic activity,[10] and that there is a correlation between the degree of activity and the amount of oxidizable cobalt in the framework.[10] Cyclohexane oxidation was also reported recently in the application of nanostructured amorphous iron and cobalt catalysts under an oxygen atmosphere. However, in these reports, leaching of the metal and recycling of the catalyst were not addressed.[15,16] In an earlier study,[17] we demonstrated that the K/A ratio could be improved by immobilizing well-defined cobalt acetate oligomers inside the pores of MCM-41, although leaching of the cobalt due to the formation of acidic side products could not be avoided. Others showed that Co could be incorporated successfully into the framework either as isolated Co^{II}[18,19] or as nanoparticles of

[a] Dr. M. S. Hamdy, Prof. Dr. J. C. Jansen
Ceramic Membrane Centre, The Pore, DelftChemTech
Technische Universiteit Delft, Julianalaan 136, 2628 BL
Delft (The Netherlands)
Fax: (+31) 15-278-4289
E-mail: J.C.Jansen@tnw.tudelft.nl

[b] Dr. A. Ramanathan, Dr. U. Hanefeld
Gebouw voor Scheikunde, Technische Universiteit Delft
Julianalaan 136, 2628 BL, Delft (The Netherlands)
Fax: (+31) 15-278-4289
E-mail: u.hanefeld@tudelft.nl

[c] Prof. Dr. T. Maschmeyer
Laboratory of Advanced Catalysis for Sustainability
School of Chemistry, The University of Sydney
NSW 2006 (Australia)

Co oxide.[20,21] The structural limitation (one-dimensional structure) of MCM-41, which affects the catalytic activity, prompted us to investigate a different heterogenization for cobalt; the incorporation into a three-dimensional, mesoporous silicate, TUD-1. In this manner, we aim to combine the improved K/A ratios of our previous studies with the advantages of framework-fixed cobalt, while avoiding the diffusion limitations that might occur in MCM-41. TUD-1 has a spongelike structure with tunable pore sizes, resulting in high substrate accessibility. In addition, the synthesis of TUD-1 is cost-effective and environmentally friendly as it is surfactant-free.[22] In an initial study, we prepared Co-TUD-1 in which the Co^{II} atoms were highly dispersed and incorporated tetrahedrally into the TUD-1 framework. With this Co-TUD-1, encouraging results were obtained in the cyclohexane oxidation.[23] Even at 5.5% cyclohexane conversion, the selectivity for mono-oxygenated products was 89% and the K/A ratio was 4.35. Moreover, no leaching and activity loss was observed. This indicated that our hypothesis was promising. Therefore, we extended our study to two types of Co incorporation into TUD-1: cobalt was incorporated into the framework or integrated as cobalt oxide particles.

Results and Discussion

Synthesis mechanism of Co-TUD-1: During the synthesis of TUD-1, triethanolamine (TEA) plays an essential role. Initially, tetraethyl orthosilicate (TEOS) was hydrolysed to produce silanol species [Eq. (1)], which then undergo partial condensation with each other and with some of the TEA [Eq. (2)] to form mixtures of mono- and oligomeric-silatrane complexes of various silica species.

$$Si(OC_2H_5)_4 + H_2O \rightarrow (C_2H_5O)_3SiOH + C_2H_5OH \quad (1)$$

$$(C_2H_5O)_3SiOH + N(CH_2CH_2OH)_3 \rightarrow N(CH_2CH_2O)_3SiOH + 3C_2H_5OH \quad (2)$$

Shan et al[24] proposed that TEA has a second role in the formation of Ti-TUD-1; to stabilize the titanium alkoxide through complexation. This is based on the observation that the three hydroxyl groups in TEA can easily replace butanol groups of Ti butoxide. Moreover, the lone-pair electrons of the nitrogen atom in TEA can be donated to the empty orbital in titanium to form stable complexes. The formation of a Co–TEA complex under the same conditions has been proven earlier.[25] The synthesis mixture thereby becomes an organic–inorganic hybrid, in which TEA and its Co complex are homogeneously dispersed in a three-dimensional silica gel.

During the drying step, a substantial loss of volatile components (water and ethanol, up to 70 wt%) takes place. At elevated temperature (hydrothermal treatment step), the silica framework will form through extensive condensation reactions between silica oligomers, and TEA and its Co complexes are expelled from the inorganic framework to form mesosized, organic-dominated aggregates.

The formation of Co–TEA complexes will lead to enriched Co species in the TEA-dominated organic phase. After calcination, Co atoms were deposited onto the internal mesoporous surface (in situ grafting). Moreover, at higher Co-loading the chance for Co_3O_4 formation increases, nanosized scale crystals will grow inside the pores, and/or bulky Co_3O_4 will be formed as extra framework crystals.

Co-TUD-1 as a mesoporous material: Figure 1a illustrates XRD patterns for the prepared Co-TUD-1 samples compared with the pattern for Co_3O_4. All Co-TUD-1 samples show a single intensive peak at low angle, indicating that Co-TUD-1 is a mesostructural material; the peak intensity decreases slightly as Co-loading increases, indicating the influence of Co-loading on the integrity of the mesoporous structure. A shift to large angles at higher Co-loading supports this observation (Figure 1b). In the spectra for Co-5 and Co-10, the peaks characteristic for crystalline Co_3O_4 become visible, indicating the presence of Co_3O_4 particles.

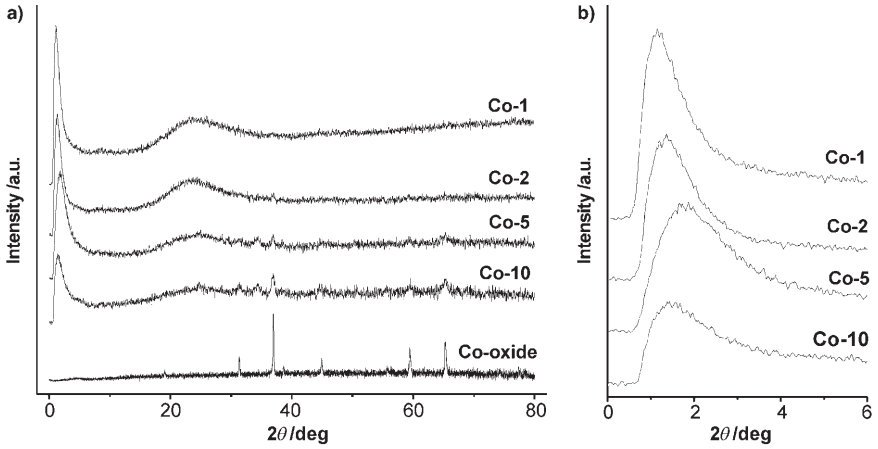

Figure 1. a) XRD patterns for Co-TUD-1 samples compared with the pattern for Co_3O_4. b) Low-angle XRD pattern of Co-TUD-1.

The elemental analysis and the porosity measurements obtained from N_2 adsorption at 77 K are listed in Table 1. Elemental analysis (Figure 2) showed that the Si/Co ratio obtained after calcination corresponds with that present in the synthesis gel, which indicates that most of the Co cations are incorporated into the final solid product. Moreover, it demonstrates the high predictability of the synthesis method.

Figure 3a shows the N_2 sorption isotherms of the Co-TUD-1 samples. All the samples show type IV adsorption isotherms, according to IUPAC classification, indicating

Table 1. Characterization of Co-TUD-1 samples with different Co-loading.

Sample	Si/Co ratio		S_{BET}[a] [m^2g^{-1}]	V_{meso}[b] [cm^3g^{-1}]	D_{meso}[c] [nm]	Color
	synthesis mixture	after calcination				
Co-1	100	108	619	0.73	4	grayish violet
Co-2	50	47.8	605	0.65	3.9	grayish violet
Co-5	20	18.6	614	0.69	3.6	gray
Co-10	10	9.95	684	0.58	3.1	gray

[a] Specific surface area. [b] Mesopore volume. [c] Mesopore diameter.

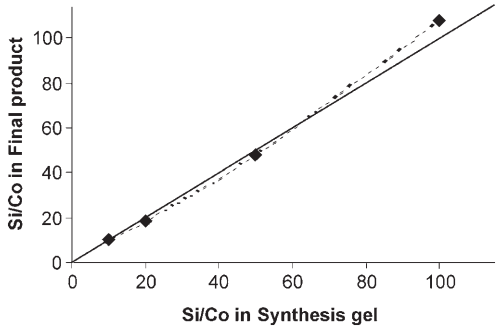

Figure 2. The elemental composition of Co-TUD-1 in the synthesis gel plotted against the Si/Co ratio obtained in the final product.

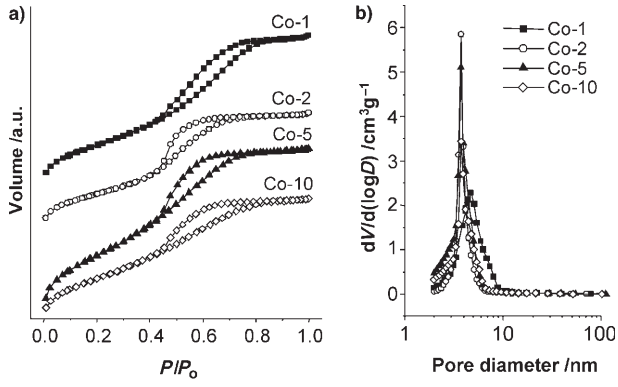

Figure 3. a) Nitrogen sorption isotherms of Co-TUD-1 samples. b) The pore-size distribution of Co-TUD-1 samples.

their mesostructured character[26] with narrow pore-size distribution (Figure 3b). All hysteresis loops exhibit the same H3-type behavior, that is, they show one well-defined step at high partial pressure ($0.45 < P/Po < 8$), which should be due to the capillary condensation of N_2 inside the mesopores. Moreover, the increase in Co-loading did not seem to affect the hysteresis type. This is an indication that the bulk crystals of Co_3O_4, which formed in samples with a higher Co-loading, were formed outside the silica framework. This is also supported by the observation that, although the surface areas did not change significantly (see Table 1), the pore volumes and pore diameters decrease as the Co-loading increases. This result is a further indication that at low Co-loading the Co is integrated into the framework of TUD-1.

The ^{29}Si magic-angle spinning (MAS)-NMR spectrum of calcined siliceous TUD-1 samples is shown in Figure 4a. After the deconvolution of the spectrum, three main peaks

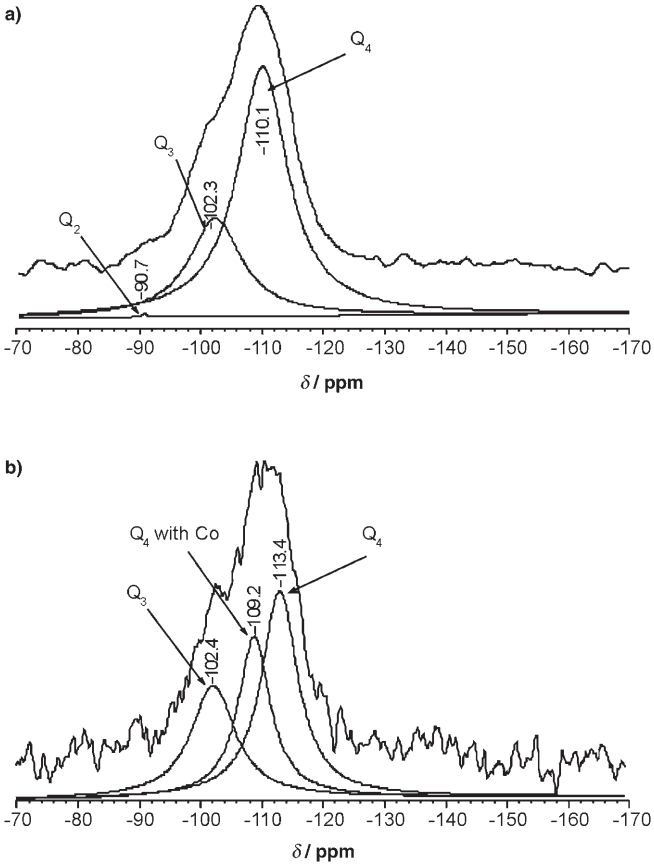

Figure 4. ^{29}Si MAS-NMR spectra for a) Si-TUD-1 compared with b) the Co-5 sample.

were detected. The first at around $\delta = -110$ ppm can be assigned to $(\text{-O-})_4\text{Si}$ with no OH group attached to the silicon atom (Q_4). The second peak at $\delta = -102$ ppm is assigned to $(\text{-O-})_3\text{Si(OH)}$ with one OH group (Q_3). The last peak at $\delta = -90$ ppm, is assigned to $(\text{-O-})_2\text{Si(OH)}_2$ with two OH groups (Q_2).[27] In contrast, in the spectrum of Co-5 (Figure 4b), three peaks were detected that show a strong paramagnetic shift due to the cobalt oxide particles/atoms incorporated into the framework. The peak at $\delta = -113$ ppm is assigned to Q_4 that was shifted due to the strong paramagnetic field of Co-oxide particles nearby, and the signal at $\delta = -102$ ppm is assigned to the Q_3. More importantly, a new signal at $\delta = -109$ ppm could be detected. This might be attributed to a Si atom adjacent to a Co atom incorporated into the TUD-1 framework as $[(\text{-O-})_3\text{Si-O-Co}]$. The ^{29}Si MAS-NMR spectra for all the samples were virtually identical: clearly the maxi-

mum of Co incorporated into the silica matrix is achieved at 1–2%, and consequently, the signal at $\delta = -109$ ppm has a similar intensity for all the samples. These conclusions are in agreement with a recent study on Co-MCM-41-like material.[28]

The UV/Vis spectra of different Co-TUD-1 samples and Co_3O_4 are presented in Figure 5. Spectra of prepared samples exhibit two peaks at around 525 and 654 nm. Both absorption bands can be assigned to the $^4A_2(F) \rightarrow {}^4T_1(P)$ transition of divalent cobalt ions (Co^{2+}) in tetrahedral coordination.[29,30] The absence of peaks at around 480 and 506 nm indicates the absence of Co^{2+} in an octahedral environment,[28,31] and the absence of a peak at 410 nm indicates the absence of framework Co^{3+}.[32] A peak at around 356 nm was detected in Co-5 and Co-10 only. This strong and broad band in the lower wavelength region will be due to the charge-transfer bands associated with the non-framework Co^{3+} species. This is strong evidence for the presence of a distinct Co_3O_4 phase, as it is the main peak found in the Co_3O_4 spectrum;[33] this is also consistent with the XRD spectra.

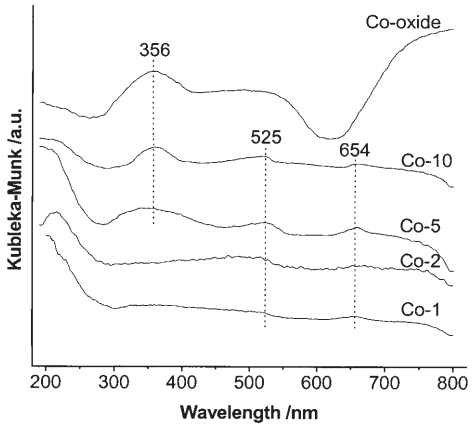

Figure 5. Diffuse reflectance UV/Vis spectra of Co-TUD-1 samples compared with that for Co_3O_4.

Laser Raman spectra of the Co-TUD-1 samples and Co_3O_4 are compared in Figure 6. All spectra showed a band at around 998 cm^{-1} that was assigned to the SiO_2 matrix.[34] The increase of the Co-loading from Co-5 to Co-10 gives rise to three bands at around 690, 485, and 525 cm^{-1}, assigned to the A_{1g}, E_g, and F_{2g} active Raman modes, respectively, of the direct spinel Co_3O_4,[35,36] which is consistent with XRD and UV/Vis spectra. The spectra for Co-1 and Co-2 were virtually identical. The broad signals at approximately 500 and 820 cm^{-1} were also described for Co-MCM-41 samples with isolated and framework-incorporated Co species at a very low Co-loading.[37]

The prepared Co-TUD-1 samples were investigated by transmission electron microscopy; almost 25 images were taken per sample. All the images of Co-1 (Figure 7) and Co-2 (not presented here) showed only the spongelike, three-dimensional structure characteristic of TUD-1 mesoporous

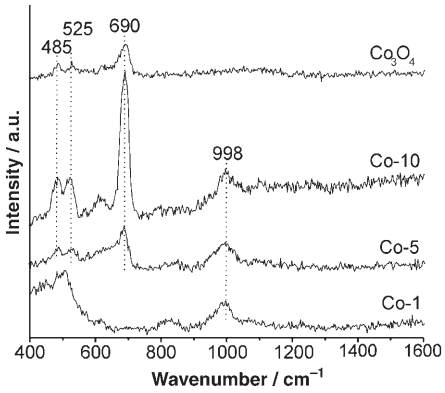

Figure 6. Laser Raman spectra of Co-TUD-1 samples compared with that of Co_3O_4. The spectrum of Co-2 is not shown as it is very similar to that of Co-1.

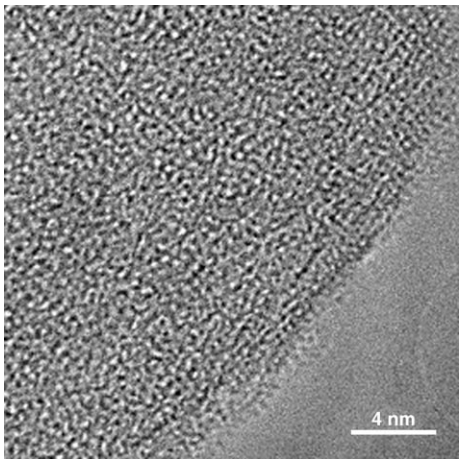

Figure 7. HRTEM image representative for the Co-TUD-1 samples. The wormlike structure of the mesoporous materials described in detail elsewhere[38] is clearly shown.

materials.[38] This is a strong indication for the incorporation of Co^{2+} ions into the framework. Given the low Co concentrations and the UV/Vis data, these Co atoms should be isolated in the framework. The images of the Co-5 sample showed also a spongelike mesoporous matrix beside the Co_3O_4 bulky crystals and, more importantly, by using higher magnification, the diffraction fringes of the embedded Co_3O_4 nanoparticles could be observed.

Table 2 summarizes the characteristics of the prepared Co-TUD-1 samples as obtained from the different characterization techniques applied.

Table 2. Appearance of Co in Co-TUD-1 samples.

Sample	Co Oxidation state	Isolated Co^{II}[a]	Co_3O_4 nanoparticles[a]	Extra framework bulky Co_3O_4[a]
Co-1	Co^{II}	++	–	–
Co-2	Co^{II}	++	–	–
Co-5	$Co^{II}+Co^{III}$	+	+	+
Co-10	$Co^{II}+Co^{III}$	+	–	++

[a] (++) abundantly present, (+) weakly or poorly present, (–) absent.

Catalysis: The major products of cyclohexane oxidation with *tert*-butylhydroperoxide (TBHP) over the Co-TUD-1 samples described above were cyclohexanone [K], cyclohexanol [A], and cyclohexylhydroperoxide (CHHP). However, trace amounts of cyclohexyl-*tert*-butylperether and cyclohexylformate were also observed as mono-oxygenated products. All the cobalt catalysts showed an excellent selectivity to mono-oxygenated products at a remarkable conversion of 5%. By comparing the results for the cyclohexane oxidation with these catalysts (Figure 8a–e), it became evident that isolated cobalt species in TUD-1 are very active in the oxidation of cyclohexane with TBHP. At the beginning of the reaction, the K/A ratios for all the cobalt catalysts studied were close to 1 or even lower (Figure 8d), and this ratio increased as conversion increased, showing that cyclohexanol [A] is the primary product, which is later oxidized to cyclohexanone [K]. A typical product distribution over Co-1 after 1 h is (mol%) K = 30.5%, A = 23.3%, CHHP = 39.0%. After 18 h, the distribution changed to K = 62.8%, A = 9.4%, CHHP = 13.7%. These values strongly indicate the oxidation of cyclohexanol to cyclohexanone with TBHP. As CHHP is one of the products formed, it might be suggested that it too can act as an oxidizing agent. However, as the conversion of cyclohexane increased from 1.2 to 10% (over Co-1), the yield of CHHP also increased continuously. This indicates that CHHP does not act as an oxidizing agent. On the other hand, it cannot be excluded that a thermal reaction, such as the mixed Russell termination[17] (Scheme 1), occurs and contributes to cyclohexanone formation. This selectivity towards cyclohexanone decreased as the loading of cobalt in the catalyst increased and is especially noticeable in Co-10, in which the cobalt is present as cobalt oxide clusters (Figure 8c and d). The loss of selectivity is accompanied by a loss of activity (Figure 8a and b). Thus, the conversion of both cyclohexane and cyclohexanol decreases as the cobalt concentration in TUD-1 increases. This might be attributed to the increasing aggregation of Co or Co oxide at higher cobalt concentrations (see above). The agglomeration of Co reduces the accessibility of the individual cobalt atoms and, therefore, of the number of active sites. At lower conversion levels, all these catalysts behaved in a similar manner, as is evident from the conversion vs selectivity graph (Figure 8e). However, at a moderate conversion of 5%, the selectivities of the catalysts show significant differences, with Co-1 being clearly the most selective catalyst (Co-1 > Co-2 > Co-5 > Co-10). Under identical experimental conditions, the cobalt oxide behaved similarly to Co-10, however, the conversions were relatively low, with CHHP as the major product (Table 3). These studies demonstrate that isolated cobalt species are more efficient than Co-oxide clusters in the oxidation of cyclohexane and cyclohexanol with TBHP.

In an earlier study,[17] we improved the K/A ratio significantly. However, overoxidation led to leaching of active cobalt species. Therefore, the aim of this study was to suppress overoxidation and the leaching of cobalt that it induces. Here, analysis for the possible overoxidation products revealed that dicarboxylic acids (adipic, succinic), monocarboxylic acids (valeric, caproic), along with very low concentrations of hydroxyacids, such as 5-hydroxyvaleric acid and 6-hydroxycaproic acid, were barely formed at low conversions. Only at higher conversions, as the selectivity of the catalysts dropped to below 93% (Figure 8e), could acids be

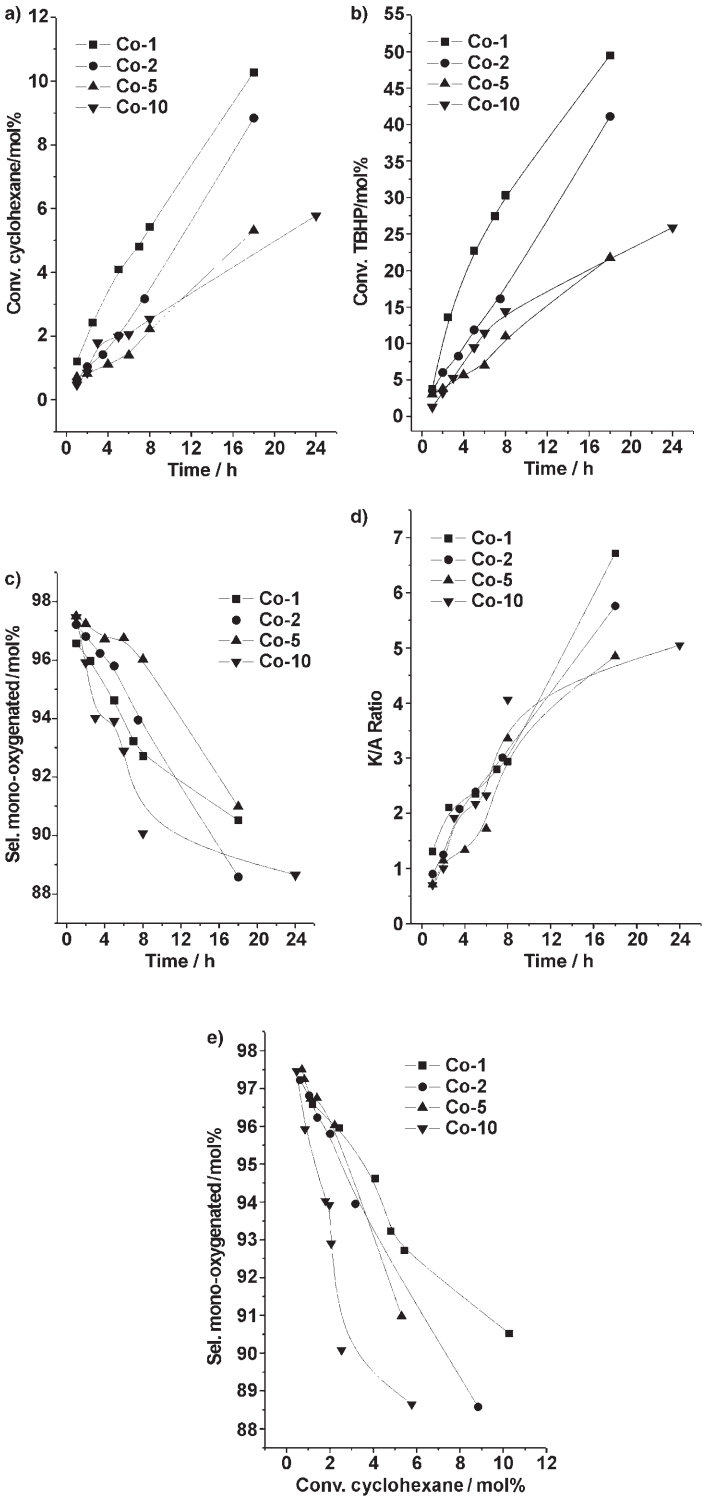

Figure 8. Catalytic performance of Co-TUD-1 samples in cyclohexane oxidation with TBHP at 70°C.

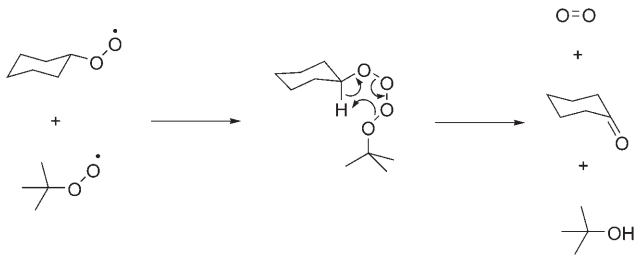

Scheme 1. Mixed Russell termination step between *t*BuOO· and *cyclo*-$C_6H_{11}OO$·.

Table 3. Cyclohexane oxidation over various Co-TUD-1 samples.

Catalyst	Time[a] [h]	Conv. cyclohexane [mol%]	Conv. TBHP [mol%]	K [%]	A [%]	CHHP [%]	Sel. mono. [mol%]	K/A ratio
Co-1	1	1.2	3.8	30.5	23.3	39	96.58	1.31
	5	4.09	22.73	45.46	19.36	26.59	92.62	2.35
	18	10.3	49.5	62.8	9.4	13.1	90.52	6.72
	3.5[b]	1.4	7.54	29.85	13.09	49.99	95.18	2.28
	24	3.40	18.76	38.78	14	37.22	94.40	2.77
Co-2	1	0.6	3.5	20.2	22.4	54.7	97.22	0.9
	7.5	3.17	16.13	31.93	10.59	46.6	93.95	3.01
	18	8.8	41.1	54.8	9.7	17.6	88.58	5.76
	4.5[b]	1.39	7.26	31.15	10.32	44.02	89.42	3.02
	21	2.90	17.71	35.5	10.08	36.15	85.71	3.5
Co-5	1	0.7	3.1	17.2	24.1	56.2	97.5	0.71
	8	2.22	10.99	30.30	9.02	56.70	96.03	3.36
	18	5.3	21.5	45.8	9.5	30.6	90.98	4.85
	4.5[b]	1.33	5.46	38.41	12.18	41.12	93.36	3.15
	24	2.69	9.16	33.49	4.67	42.3	84.9	3.74
Co-10	1	0.5	1.3	18.3	26.2	50.1	97.46	0.7
	8	2.54	14.39	35.32	8.33	44.04	90.08	4.24
	24	5.8	25.9	49. 3	9.8	27.1	88.65	5.05
	4[b]	1.52	8.31	35.14	11.69	39.13	88.5	3.01
	24	2.97	13.0	27.75	5.8	45.24	83.8	4.78
Co_3O_4	1	0.34				76	–	–
	18	2.0				69	–	–

[a] Total reaction time. [b] Analysis from hot-filtration studies.

observed. To confirm that the catalysts are indeed heterogeneous and that no activity leaches, hot-filtration studies were performed. After 1 h of reaction, the hot (above 50 °C) reaction mixture was filtered, and the reaction was continued with the filtrate. The results (Table 3) indicate that, after a period of 2–5 h, there is still a low level of activity in the filtrate, due to the slow termination of residual radical chains. However, after longer runs (24 h), there is little improvement in the conversion of cyclohexane. The heterogeneity of this reaction was further reflected in the drop in selectivity for mono-oxygenated products at comparable conversion levels. Analysis of the Co-TUD-1 samples for their Co content after filtration revealed no loss of metal. This once again suggests that Co is incorporated into the TUD-1 framework.

Conclusion

We have demonstrated the application of cobalt-containing, three-dimensional mesoporous silicate, Co-TUD-1, in the oxidation of cyclohexane. Improvements in the selectivity for mono-oxygenated products, as well as in the K/A ratio, were achieved. Cobalt was successfully incorporated into the three-dimensional silica matrix of TUD-1 either as isolated Co atoms or as bulky cobalt oxide particles. At lower concentrations, the cobalt is incorporated into the framework of TUD-1 as an isolated atom, whereas at higher loading of cobalt, oxide clusters along with a very small amount of cobalt oxide nanoparticles are observed in the TUD-1. This new catalyst system is heterogeneous, as no catalytic activity was detected after hot filtration.

Experimental Section

Materials synthesis: Co-TUD-1 samples with different Co content (Si/Co ratio = 100, 50, 20, and 10 denoted as Co-1, Co-2, Co-5, and Co-10, respectively) were synthesized by means of direct hydrothermal treatment (DHT) according to the molar oxide ratio SiO_2:x CoO:0.5 TEAOH:1 TEA:11 H_2O (TEAOH = tetraethyl ammonium hydroxide). In a typical synthesis (for Co-1),[23] a mixture of 12.6 g TEA (97%, ACROS) and deionized water (3.5 mL) was added drop-wise to a mixture of 17.4 g tetraethyl orthosilicate (TEOS, >98%, ACROS) and 0.23 g cobalt(II)sulfate heptahydrate ($CoSO_4 \cdot 7H_2O$, Aldrich) dissolved in deionized water (5 mL) under vigorous stirring. After stirring for a further 30 min, 10.3 g of TEAOH (35%, Aldrich) was added. The mixture was aged at RT for 24 h, dried at 100 °C for 24 h, and then hydrothermally treated in teflon-lined stainless steel autoclaves at 180 °C for 4 h. Finally, the solid samples were calcined at 600 °C for 10 h at a ramp rate of 1 °C min^{-1} in air.

Materials characterization: Powder X-ray diffraction (XRD) patterns were measured by using a Philips PW 1840 diffractometer equipped with a graphite monochromator using $Cu_{K\alpha}$ radiation ($\lambda = 0.1541$ nm). The samples were scanned over a range of 0.1–80° 2θ with steps of 0.02°. Nitrogen adsorption and desorption isotherms were recorded by using a QuantaChrome Autosorb-6B at 77 K. The pore-size distribution was calculated from the adsorption branch by using the Barret–Joyner–Halenda (BJH) model.[39] Samples were previously evacuated at 623 K for 16 h. The BET method was used to calculate the surface area (S_{BET}) of the samples, and the mesopore volume (V_{meso}) was determined by using the *t*-plot method according to Lippens and de Boer.[40] Instrumental neutron activation analysis (INAA)[41] for chemical composition determination (elemental analysis) was performed by using the "Hoger Onderwijs Reactor" nuclear reactor with a thermal power of 2 MW and maximum neutron reflux of 2×10^{14} $m^{-2} s^{-1}$. This method can be applied to solid samples and was used because of difficulties in dissolving the samples. The method proceeds in three steps: irradiation of the elements with neutrons in the nuclear reactor, a period of decay, and finally, measurement of the

radioactivity resulting from irradiation. The energy of the radiation and the half-life period of the radioactivity enable a highly accurate quantitative analysis.[41] ^{29}Si MAS-NMR experiments were performed at a magnetic field of 9.4 T by using a Varian VXR-400 S spectrometer operating at 104.2 MHz with pulse width of 3.2 msec. Zirconia rotors of 4 mm were used with a spinning speed set to 8 kHz. The chemical shift was measured with respect to tetraethylsilane (TMS) as an external standard at 0 ppm. 1000 scans were collected by using a sweep width of 20000 Hz and an aquisition delay of 20 sec.

UV/Vis spectra were collected at ambient temperature by using a Cary-Win 300 spectrometer with $BaSO_4$ as a reference. Samples were ground carefully, heated overnight at 180 °C, and then scanned from 190–800 nm. The UV/Vis absorption data were converted to Kubelka–Munk units. The in situ laser Raman spectra were obtained by using a Renishaw Raman Imaging Microscope, system 2000. The green ($\lambda = 514$ nm) polarized radiation of an argon-ion laser beam of 20 mW was used for excitation. A Leica DMLM optical microscope with a Leica PL floutar L500/5 objective lens was used to focus the beam onto the sample. The Ramascope was calibrated by using a silicon wafer. Samples were dehydrated in situ in an air flow of 100 mL min^{-1} by using a temperature-programmed heated cell (Linkam TS1500). The spectra were collected in the range of 180–1600 cm^{-1}. HRTEM was carried out by using a Philips CM30UT electron microscope with a field-emission gun as the source of electrons operated at 300 kV. Samples were mounted on a copper-supported carbon-polymer grid by placing a few droplets of a suspension of ground sample in ethanol onto the grid, followed by drying under ambient conditions. Electron dispersive X-ray (EDX) elemental analysis was performed by using a LINK EDX system. Atomic absorption spectroscopy (AAS) analysis for leached metal ions in the filtered product mixtures of cyclohexane oxidation experiments was performed by using a Perkin–Elmer 4100ZL instrument.

Catalytic performance: A stock solution of TBHP in cyclohexane was prepared by extraction of commercial TBHP (Aldrich, 70% in water) into an equal volume of cyclohexane. Phase separation was promoted by saturation of the aqueous layer with NaCl. The organic layer was dried over $MgSO_4$, filtered, and stored at 4 °C. TBHP content was determined by GC analysis with chlorobenzene as an internal standard.

Oxidation of cyclohexane was carried out with 20 mL of a mixture of cyclohexane (65 mol%) and TBHP (35 mol%). Chlorobenzene (1 g) was added as the internal standard. In all the experiments, an equimolar concentration of cobalt was used (0.1 mmol). The round-bottomed glass flask with the reaction mixture containing the catalyst was then immersed in a thermostated oil bath. The gas phase above the reaction mixture was filled with nitrogen and a gas burette was attached. The course of the reaction was followed by analyzing the liquid samples with a gas chromatograph (Agilent 6890) equipped with a split inlet (200 °C, split ratio 10.0) and a Sil 5 CB capillary column (ID, 50 m × 0.53 mm; constant flow of carrier gas N_2, 4.0 mL min^{-1}) coupled to a FID detector. The concentration of carboxylic acid side products was determined by performing GC analysis from separate samples after conversion into the respective methyl esters.[17,23] Identification of the products was achieved by conducting GC–MS. The evolution of molecular oxygen and its consumption was monitored volumetrically by using the attached gas burette. The conversion of cyclohexane is defined in mol%, that is, the number of moles of products formed divided by the initial number of moles of cyclohexane multiplied by 100. All mass balances were >92%.

Acknowledgements

U.H. thanks the Royal Netherlands Academy of Arts and Sciences (KNAW) for a fellowship. M.S.H. thanks Helwan University and the Ministry of Higher Education of the Egyptian Government for a fellowship. The authors are thankful to Delia van Rij for carrying out INAA analysis, Sander Brouwer for N_2 sorption experiments, and Kristina Djanashvili for NMR analysis.

[1] W. B. Fisher, J. F. Van Peppen in *Kirk Othmer Encyclopedia of Chemical Technology*, 4th ed., Vol. *7* (Ed.: M. Howe-Grant), Wiley, New York, **1996**, pp. 859–871.
[2] M. T. Musser in *Ullmann's Encyclopedia of Industrial Organic Chemicals*, Vol. *3*, VCH-Wiley, Weinheim, **1999**, pp. 1807–1821.
[3] P. A. MacFaul, I. W. C. E. Arends, K. U. Ingold, D. D. M. Wayner, *J. Chem. Soc. Perkin Trans 2* **1997**, 135–145.
[4] R. A. Sheldon, J. K. Kochi, *Metal-Catalyzed Oxidation of Organic Compounds*, Academic Press, New York, **1981**, Chapter 11.
[5] P. Tian, Z. Liu, Z. Wu, L. Xu, Y. He, *Catal. Today* **2004**, *93–95*, 735–742.
[6] S. K. Mohapatra, P. Selvam, *Top. Catal.* **2003**, *22*, 17–22.
[7] A. F. Masters, J. K. Beattie, A. L. Roa, *Catal. Lett.* **2001**, *75*, 159–162.
[8] R. Raja, G. Sankar, J. M. Thomas, *J. Am. Chem. Soc.* **1999**, *121*, 11926–11927.
[9] D. L. Vanoppen, P. A. Jacobs, *Catal. Today* **1999**, *49*, 177–183.
[10] G. Sankar, R. Raja, J. M. Thomas, *Catal. Lett.* **1998**, *55*, 15–23.
[11] I. Belkhir, A. Germain, F. Fajula, E. Fache, *J. Chem. Soc. Faraday Trans.* **1998**, *94*, 1761–1764.
[12] F. J. Luna, S. E. Ukawa, M. Wallau, U. Schuchardt, *J. Mol. Catal. A* **1997**, *117*, 405–411.
[13] D. L. Vanoppen, D. E. De Vos, M. J. Genet, P. G. Rouxhet, P. A. Jacobs, *Angew. Chem.* **1995**, *107*, 637–639; *Angew. Chem. Int. Ed. Engl.* **1995**, *34*, 560–563.
[14] S.-S. Lin, H.-S. Weng, *Appl. Catal. A* **1993**, *105*, 289–308.
[15] N. Perkas, Y. Koltypin, O. Palchik, A. Gedanken, S. Chandrasekaran, *Appl. Catal. A* **2001**, *209*, 125–130.
[16] V. Kesavan, P. S. Sivanand, S. Chandrasekaran, Y. Koltypin, A. Gedanken, *Angew. Chem.* **1999**, *111*, 3729–3730; *Angew. Chem. Int. Ed.* **1999**, *38*, 3521–3523.
[17] M. Nowotny, L. N. Pedersen, U. Hanefeld, T. Maschmeyer, *Chem. Eur. J.* **2002**, *8*, 3724–3731.
[18] V. Parvulescu, B. L. Su, *Catal. Today* **2001**, *69*, 315–322.
[19] S. Lim, D. Ciuparu, C. Pak, F. Dobek, Y. Chen, D. Harding, L. Pfefferle, G. Haller, *J. Phys. Chem. A* **2003**, *107*, 11048–11056.
[20] D. Dhar, Y. Koltypin, A. Gedanken, S. Chandrasekaran, *Catal. Lett.* **2003**, *86*, 197–200.
[21] J. Haskouri, S. Cabrera, C. Guillem, J. Latorre, A. Beltran, M. D. Marcos, C. J. Gomes-Garcia, D. Beltran, P. Amoros, *Eur. J. Inorg. Chem.* **2004**, *9*, 1799–1803.
[22] J. C. Jansen, Z. Shan, L. Marchese, W. Zhou, N. van der Puil, T. Maschmeyer, *Chem. Commun.* **2001**, 713–714.
[23] R. Anand, M. S. Hamdy, U. Hanefeld, T. Maschmeyer, *Catal. Lett.* **2004**, *95*, 113–117.
[24] Z. Shan, E. Gianotti, J. C. Jansen, J. A. Peters, L. Marchese, T. Maschmeyer, *Chem. Eur. J.* **2001**, *7*, 1437–1443.
[25] S. Teller, Y. Marcus, Y. Tur'Yan, *Polyhedron* **1997**, *16*, 1047–1056.
[26] K. S. W. Sing, D. H. Everett, R. A. W. Haul, L. Moscou, R. A. Pierotti, J. Rouquerol, T. Siemieniewska, *Pure Appl. Chem.* **1985**, *57*, 603–619.
[27] K. J. Mackenzie, M. E. Smith in *Multinuclear Solid-State NMR of Inorganic Materials*, Pergamon, **2002**.
[28] J. Haskouri, S. Cabrera, C. J. Gomes-Garcia, C. Guillem, J. Latorre, A. Beltran, D. Beltran, M. D. Marcos, P. Amoros, *Chem. Mater.* **2004**, *16*, 2805–2813.
[29] J. Sponer, J. Cejka, J. Dedecek, B. Wichterlova, *Microporous Mesoporous Mater.* **2000**, *37*, 117–127.
[30] R. S. da Cruz, A. J. S. Mascarenhas, H. M. C. Andrade, *Appl. Catal. B* **1998**, *18*, 223–231.
[31] J. Y. Yan, M. C. Kung, W. M. Sachtler, H. H. Kung, *J. Catal.* **1997**, *172*, 178–186.
[32] W. A. Carvalho, P. B. Varaldo, M. Wallau, U. Schuchardt, *Zeolite* **1997**, *18*, 408–416.
[33] E. Finocchio, T. Montanari, C. Resini, G. Busca, *J. Mol. Catal. A* **2003**, *204–205*, 535–544.
[34] C. Wang, G. Deo, I. E. Wachs, *J. Catal.* **1998**, *178*, 640–648.

[35] M. A. Stanick, M Hoalla, D. M. Hercules, *J. Catal.* **1987**, *106*, 362–362.
[36] H. Jeziorowski, H. Knoezinger, P. Grange, P. Gajardo, *J. Phys. Chem.* **1980**, *84*, 1825–1829.
[37] Q. Tang, Q. Zhang, H. Wu, Y. Wang, *J. Catal.* **2005**, *230*, 384–397.
[38] P. Waller, Z. Shan, L. Marchese, G. Tartaglione, W. Zhou, J. C. Jansen, T. Maschmeyer, *Chem. Eur. J.* **2004**, *10*, 4970–4976.
[39] E. P. Barrett, L. G. Joyner, P. P. Halenda, *J. Am. Chem. Soc.* **1951**, *73*, 373–380.
[40] B. C. Lippens, J. H. de Boer, *J. Catal.* **1965**, *4*, 319–323.
[41] F. Boynton in *Handbook on the Physics and Chemistry of Rare Earths, Vol. 4* (Eds.: K. Gschneidner, Jr., L. Eyring), North-Holland Publishing Company, Amsterdam, **1979**, pp. 457–470.

Received: February 15, 2005
Revised: August 8, 2005
Published online: December 6, 2005

